

PREDICTION OF HEAT GENERATION IN RUBBER OR RUBBER-METAL SPRINGS

by

**Milan S. BANIĆ^{a*}, Dušan S. STAMENKOVIĆ^a, Vojislav Dj. MILTENOVIĆ^a,
Miloš S. MILOŠEVIĆ^a, Aleksandar V. MILTENOVIĆ^a, Petar S. DJEKIĆ^a,
and Milan J. RACKOV^b**

^aFaculty of Mechanical Engineering, University of Niš, Niš, Serbia

^bFaculty of Technical Sciences, University of Novi Sad, Novi Sad, Serbia

Original scientific paper
DOI: 10.2298/TSCI120503189B

The temperature of rubber or rubber-metal springs increases under cyclic loading, due to hysteresis losses and low rubber thermal conductivity. Hysteresis losses correspond to energy dissipation from the rubber, which is primarily converted into heat. This well-known phenomenon, called heat build-up, is the primary reason for rubber aging. Increase in temperature within the rubber compound leads to degradation of its physical and chemical properties, increase in stiffness and loss of damping capability. This paper presents a novel procedure of heat generation prediction in rubber or rubber-metal springs. The procedure encompasses the prediction of hysteresis loss, i. e. dissipated energy within the rubber, by finite element analysis and application of a modern visco-plastic rubber constitutive model. The obtained dissipated energy was used as an input for transient thermal analysis. Verification of the proposed procedure was performed by comparison of simulation results with experimentally obtained data during the dynamic loading of the rubber specimen. The proposed procedure is highly computationally efficient and it enables time integration, which can be problematic in coupled mechanical thermal analysis.

Key words: *rubber-metal spring, hysteresis heat generation, finite elements analysis*

Introduction

Rubber or rubber-metal springs are widely used as anti-vibration or anti-shock components in technical systems. Their basic advantages in respect to metal ring springs are: lower price, easier installation, lower mass (six times lighter for the same dynamic capacity), reduced corrosion, no risk of fracture, and no need for lubrication [1]. However, the basic disadvantage of rubber or rubber-metal springs is an insufficiently reliable service life caused by rubber fatigue.

When rubber is used for a long period of time it ages, becomes stiffer and loses its damping capability. This aging process results mainly from heat generated within the rubber

* Corresponding author; e-mail: banic@masfak.ni.ac.rs

due to hysteresis loss, and it affects the material properties, as well as the useful lifetime of rubber [2].

Due to the viscoelastic response of the rubber compounds, stress-strain curve of the rubber creates a hysteretic loop during the full load-unload cycle. The area in hysteresis loop corresponds to dissipated energy which is primarily converted into heat [3, 4]. Since heat generation occurs within the material and it is not easily conducted away due to rubber thermal properties, heat generation causes an increase in temperature inside the rubber compound which can even lead to melting of the material or to explosive rupture (blowout).

Heat generation in rubber compounds is affected by the nature of polymers, the physical and chemical properties of the compounding ingredients, their interaction with rubber, operating parameters, and the environment [5]. The decrease in heat generation of rubber or rubber-metal springs leads to their longer service life.

As hysteresis heat generation is a major concern to rubber lifetime, numerous authors have researched the processes of heat generation in rubber compounds, as well as the effect of heat generation on rubber lifetime and its thermo-mechanical properties. Recently, several authors applied the numerical approach to predict hysteresis heat generation.

Pesek *et al.* [3] proposed a mathematical model based on weak formulation of partial differential equation by finite element method (FEM) to investigate the thermo-mechanical interaction in pre-stressed rubber block used for resilient elements of the composed tram wheels. The authors used a proportional damping model and conservative energy law, *i. e.* equality of heat energy density and dissipation energy density, to perform coupling between the mechanical and thermal equations under selected simple stress states, such as uniaxial tension and/or compression or pure shear. Besides using the simple load cases and assumed damping model, the authors did not experimentally validate the proposed mathematical model at different strain rates.

Luo *et al.* [6] based their finite elements analysis (FEA) approach on experimentally obtained static hysteresis loop to predict heat generation of Instrumount rubber spring during the spring accelerated fatigue tests. The experimentally obtained static hysteresis loop was used to calculate energy loss per cycle. The authors determined that energy loss per cycle of the rubber spring loading, under fixed dynamic amplitude, did not depend on the loading frequency. Lin *et al.* [7] used similar approach to perform steady-state thermal analysis of a rolling tire. Their approach to the problem consisted in determination of specimen hysteresis by dynamic mechanical analyzer (DMA) and total mechanical energy by FEA with a hyperelastic constitutive model. The dissipated energy was obtained as a product of obtained hysteresis and total mechanical energy of hyperelastic material. Lin also concluded that hysteresis loss had similar values at different frequencies, especially when the temperature was above 25 °C.

The procedures proposed by the authors in [6] and [7] require experimental determination of hysteresis loss at all amplitudes, *i. e.* strain values at which spring operates which can be quite problematic and time consuming.

Johnson *et al.* [4] used the visco-elastic (Maxwell solid) model to estimate hysteresis loss and to predict heat generation in rubber compounds. Although the proposed approach was purely numerical, addressing the abovementioned necessity to experimentally determine hysteresis loss, the accuracy of the proposed approach decreased radically with strain and frequency increase. For instance, the error in dissipated energy prediction at strain value of 0.5 was above 35%, which is unacceptable for capturing of heat generation in rubber component. Due to full coupling of the mechanical and thermal analysis, the proposed approach addressed only moderate temperature changes and did not discuss time-temperature superposition. Fur-

thermore, the proposed approach could not capture Mullins effect, *i. e.* stress softening of rubber compounds which has a great effect on compound mechanical behavior.

Modern visco-plastic constitutive models, such as Bergstrom-Boyce model, are very effective at predicting the average behavior of an elastomer, as well as the rate-effect, dynamic loading, hysteresis behavior, and Mullins effect. The aim of this paper is to propose an efficient procedure for prediction of heat generation in rubber or rubber-metal springs by application of visco-plastic material model augmented with rubber damage model in FEA. The proposed procedure encompasses the prediction of dissipated energy during the cycling loading. The dissipated energy was then used as an input for transient thermal analysis in which component temperature distribution was obtained. The proposed approach was verified by comparison of simulation results with experimentally obtained temperature distribution. The overview of modern visco-plastic constitutive model is also given to facilitate the description of dissipated energy prediction, as well as the procedure for determination of parameters of the used rubber constructive model.

Definition of heat generation prediction procedure

Although modern commercial FE packages are capable of performing full coupling of mechanical and thermal fields as proposed in [3, 5], such an approach is highly inefficient when time-temperature superposition is demanded due to huge computational demands, especially in springs with complicated geometry. To overcome the noted problem, the procedure for prediction of heat generation due to hysteresis loss in rubber or rubber-metal springs is proposed. A schematic (algorithm) of this novel procedure is shown in fig. 1. The proposed procedure is similar to the procedure given in [6], but instead of experimental determination of static hysteresis, it is determined by computer simulation (FEM). The determination of static hysteresis (I) is enabled by the application of a visco-plastic rubber constitutive model. If assumed that dissipated energy (E_D) is primarily converted into heat, the heat generation rate (H_G) can be derived from static hysteresis and total mechanical energy (E_T) or total mechanical energy and absorbed energy (E_R) as:

$$H_G = \frac{E_D}{t} = \frac{IE_T}{t} = \frac{E_T - E_R}{t} \quad (1)$$

Due to relatively low computational demands, the proposed approach enables the time integration, thus enabling the prediction of spring heat emission during prolonged operation time, *i.e.* establishing of thermal equilibrium.

A review of accuracy [8] of predictive capabilities of modern constitutive theories for filled elastomers clearly indicates that the best accuracy is obtained by usage of a visco-plastic material model augmented with a rubber damage model. Relative prediction error of hyperelastic models, usually applied to predict behavior in commercial FE codes, increases

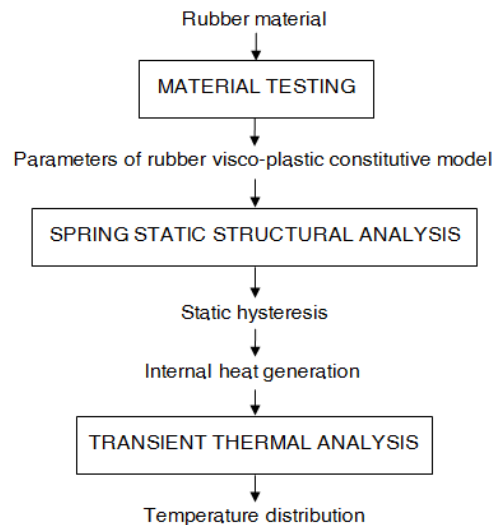


Figure 1. A schematic for new procedure for temperature distribution prediction in rubber and rubber-metal springs with FEA

with the increase in particle filler percentage of rubber compound and can go up to 45% at moderate filler percentages. The relative prediction error of a widely used visco-plastic Bergstrom-Boyce constitutive model [8] augmented with Ogden-Roxburgh Mullins damage model (Bergstrom-Boyce-Mullins – BBM) is within 2%, and it is relatively insensitive to filler percentage.

The high accuracy across different elastomer compounds of BBM damage model was a primary reason for adaptation of the noted material model during investigation of heat generation in rubber or rubber-metal springs due to hysteresis loss.

Constitutive modeling

Commercial finite elements (FE) packages are delivered with a selection of material models that are suitable for elastomers, primarily hyperelastic models. Hyperelastic models are effective at predicting the average behavior of an elastomer, but do not capture rate-effects, dynamic loading, hysteresis, or Mullins effect. Visco-elastic or visco-plastic material models which can predict the rate-effect, dynamic loading, and hysteresis behavior are available only in several commercial FE packages. Augmenting of hyperelastic or visco-elastic/plastic models with a rubber damage model is only available through user material, so it is necessary to give an overview of governing equations necessary for implementation of user material.

The Bergstrom-Boyce material model is a phenomenologically based, highly nonlinear model used to model visco-plastic behavior of elastomers. The model allows for a nonlinear stress-strain relationship, strain rate dependence and can capture the hysteresis effect of elastomers. The time dependent behavior of realistic rubber compounds (or elastomers) can be mechanically described by decoupling it into two parts: an equilibrium response and time dependent deviation from the equilibrium response [10]. Rubber compounds or elastomers can then be modeled as two parallel polymer networks (fig. 2). The first network (A) captures the equilibrium response and can be modeled by using any of the known hyperelastic material models. The second network (B) represents a perfect network in series with a time dependent element which acts to relieve the strain in the network over time.

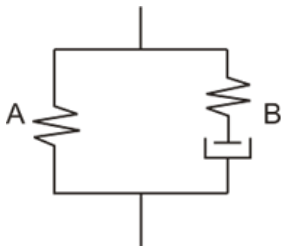


Figure 2. One-dimensional representation of Bergstrom-Boyce rheological constitutive model of elastomers [10]

The deformation gradient \mathbf{F} acts on both networks so it can be represented as [10]:

$$\mathbf{F} = \mathbf{F}_A = \mathbf{F}_B = \nabla_{\mathbf{x}} \mathbf{x} \quad (2)$$

The deformation gradient of the time dependent network (B) \mathbf{F}_B can be further decomposed to elastic \mathbf{F}_{Be} and inelastic \mathbf{F}_{Bi} parts [11]:

$$\mathbf{F}_B = \mathbf{F}_{Be} \mathbf{F}_{Bi} \quad (3)$$

The stress in network A (\mathbf{T}_A) can be obtained from the 8-chain network model given by Arruda *et al.* [10]:

$$\mathbf{T}_A = \frac{\mu_A^0}{J_A \lambda_A^*} \frac{\mathcal{L}^{-1} \left(\frac{\overline{\lambda}_A^*}{\lambda_A^{lock}} \right)}{\mathcal{L}^{-1} \left(\frac{1}{\lambda_A^{lock}} \right)} \text{dev} [\mathbf{B}_A^*] + K J_A^{-1} \mathbf{I} \quad (4)$$

where

$$\mathbf{B}_A^* = \frac{1}{\sqrt[3]{J_A^2}} \mathbf{F} \mathbf{F}^T \quad (5)$$

$$\overline{\lambda}_A^* = \sqrt{\frac{\text{tr}(\mathbf{B}_A^*)}{3}} \quad (6)$$

$$J_A = \det \mathbf{F} \quad (7)$$

$$\mathcal{L} = \coth(x) - \frac{1}{x} \quad (8)$$

The initial shear modulus of the equilibrium network (μ_0^A) and limiting stretch of the equilibrium network (λ_A^{lock}) are the material constants, which are determined experimentally.

The stress in the elastic part of network B can be obtained similarly as stress in network A, by the 8-chain network model:

$$\mathbf{T}_B = \frac{\mu_B^0}{J_{Be} \lambda_{Be}^*} \frac{\mathcal{L}^{-1} \left(\frac{\overline{\lambda}_{Be}^*}{\lambda_{Be}^{lock}} \right)}{\mathcal{L}^{-1} \left(\frac{1}{\lambda_{Be}^{lock}} \right)} \text{dev} [\mathbf{B}_{Be}^*] + K J_{Be}^{-1} \mathbf{I} \quad (9)$$

The components of eq. (9) are analogous to components of eq. (4) and they are computed in the same way as for eq. (4). The initial shear modulus of the time depended network (μ_B^0) and limiting stretch of the time depended network (λ_B^{lock}) are the material constants, which are determined experimentally.

The viscous deformation of network B can be found from the total deformation and elastic deformation:

$$\mathbf{F}_{Bi} = \mathbf{F}_{Be}^{-1} \mathbf{F} \quad (10)$$

Correct solutions for components of the time dependent network will satisfy the eq. [10]:

$$\dot{\mathbf{D}}_{Bi} = \dot{\gamma}_B \mathbf{N}_B \quad (11)$$

The effective creep rate ($\dot{\gamma}_B$) can be defined as [9]:

$$\dot{\gamma}_B = \dot{\gamma}_0 \left[\overline{\lambda}_{Be}^* - 1 + \xi \right]^C \left[R \left(\frac{\tau_B}{\tau_B} - \hat{\tau}_{cut} \right) \right]^m \quad (12)$$

where $\dot{\gamma}_0 \equiv 1 \text{ s}^{-1}$ is a dimensional consistency constant, $R(x) = (x + |x|)/2$ – the ramp function, $\hat{\tau}_{cut}$ – the cut off stress (below which no viscous flow occur), and $\hat{\tau}_B$, $m \in \mathbb{R}^+$ and $C \in [0, -1]$ are the material constants, which are determined experimentally.

The total stress in the model can be expressed as:

$$\mathbf{T} = \mathbf{T}_A + \mathbf{T}_B \quad (13)$$

To account for the Mullins effect, Ogden and Roxburgh proposed an extension of hyperelastic models in which the strain energy density, U , is taken to be a function not only of the applied deformation state, but also an internal state variable η , tracking the damage state in the material [8].

The eight-chain hyperelastic network A (fig. 2) includes the damage term η , so the total stress in the model can be expressed as [12]:

$$\mathbf{T} = \eta \mathbf{T}_A + \mathbf{T}_B \quad (14)$$

For incompressible loading, the following form is used [8]:

$$U(\lambda_1, \lambda_2, \lambda_3, \eta) = \eta U(\lambda_1, \lambda_2, \lambda_3) \quad (15)$$

where λ_i are the principal stretches. In the Ogden-Roxburgh model the damage variable is taken to evolve with applied deviatoric strain energy as follows [12]:

$$\eta = 1 - \frac{1}{r} \operatorname{erf} \left(\frac{U_{dev}^{\max} - \alpha U_{dev}}{\hat{U} + \beta U_{dev}^{\max}} \right) \quad (16)$$

$$U_{dev}^{\max} = \max \left[\alpha U_{dev}, U_{dev}^{\max} \right] \quad (17)$$

$$\alpha = \max \left[\alpha_{\min}, \left(\frac{U_{dev}^{\min}}{U_{dev}^{\max}} \right)^b \right] \quad (18)$$

$$U_{dev}^{\min} = \begin{cases} U_{dev}^{\max} & , \text{ if } \alpha U_{dev} \geq U_{dev}^{\max} \\ \min \left[\alpha U_{dev}, U_{dev}^{\min} \right] & , \text{ otherwise} \end{cases} \quad (19)$$

where \hat{U} , r , α_{\min} and β are material parameters which are determined experimentally, $\operatorname{erf}(x)$ is the error function, U_{dev} is the current deviatoric strain energy density, and $U_{dev}^{\min} / U_{dev}^{\max}$ are the evolving minimum/maximum deviatoric strain energies.

Procedure verification

In order to verify the proposed procedure for prediction of heat generation due to hysteresis losses (fig. 1) the case study was defined. The goal of the case study was to obtain temperature of the rubber specimen uniaxially compressed between two steel plates to approximately 45% at 2.2 Hz.

The rubber mixture for verification procedure was selected according to the boundary criterion, *i. e.* based on the assumption of the lowest prediction accuracy. As prediction

accuracy of all constitutive models decreases with the increase in filler amount [8, 13], the high filler percentage compound was selected for validation purposes. Furthermore, as available literature provides a lot of data about prediction accuracy of various types of elastomers, the rubber compound was chosen according to the criterion of the least available data about prediction accuracy. Based on the abovementioned criteria, the rubber mixture with the trade name TG-B-712 by manufacturer “TIGAR technical rubber” from Serbia was selected. TG-B-712 is a caoutchouc-butyl rubber with vol40% carbon black particles. Mechanical properties of TG-B-712 are given in tab. 1.

Table 1. Mechanical properties of rubber compound TG-B-712 [9]

Test	
Hardness in Sh-A according to ISO/48	80
Strength in MPa according to ISO/37	15.3
Elongation at rupture in % according to ISO/37	379
200% modulus of elasticity in MPa according to ISO/37	9
Compression set after 25% compression for 24 hours at 70 °C in % according to ISO/815	12.1

The heat generation was predicted according to the proposed procedure and then compared with the experimentally obtained distribution. During the verification procedure, the simulation prediction of temperature distribution followed exactly the experimental procedure in regard to loading and boundary conditions. Furthermore, the force-displacement data was recorded during the experimental investigation in order to verify the accuracy of the applied BBM constitutive model at strain rates different than the one used during the model parameters determination.

The compression of the specimen was performed at an eccentric mechanical press for the time period of 1 hour. The experimental setup is shown in fig. 3. Two pieces of high granulation sandpaper were inserted between the rubber specimen and compression plates during the experimental verification, in order to eliminate the influence of friction on the prediction of static hysteresis. Such friction condition enables the approximation of interface between the rubber and metal plates as they are bonded. Furthermore, insertion of sandpaper between the rubber specimen and the compression plates provides thermal isolation of the rubber specimen [14]. The temperature measurement in experimental verification was performed by a K-type thermocouple and a JENOPTIC model Varioscan 3021ST infrared camera. The K-type thermocouple was inserted into the center of rubber specimen through a previously drilled hole with the diameter of 2 mm.



Figure 3. Experimental set-up during verification procedure

The infrared camera captured the temperature of rubber surface at equal time intervals of 30 seconds. During thermography, the emissivity value of 0.95 was used [15], so the temperatures of compression plates could not be determined from the thermal camera images.

Determination of model parameters

In order to determine material constants of the above described Bergstrom-Boyce-Mullins model, several experiments were performed on rubber samples.



Figure 4. A rubber sample in a compressed state at true strain value of -1.1

All the experiments were performed in the uniaxial compression at different strain rates on the samples of the chosen rubber compound ($\varnothing 35.7 \times 17.8$ mm). The samples were compressed between hardened steel plates. As friction has a great influence in compression experiments [16, 17], barreling of samples was prevented by lubrication of the compression plates with machine oil (fig. 4). All tests were conducted on a uniaxial testing machine, whose support plates contained a spherical seat for alignment of the sample and compression plates.

The samples were conditioned by five load cycles to a final true strain of about -1.1 . The testing was conducted at strain rates of $-0.085/s$ and $-0.55/s$ (fig. 5). The stress relaxation test during the uniaxial compression (fig. 6) was also performed in order to determine the necessary model parameters of the time dependent network.

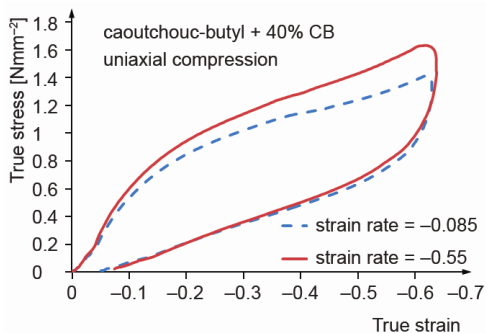


Figure 5. Stress-strain response of the rubber sample at different strain rates

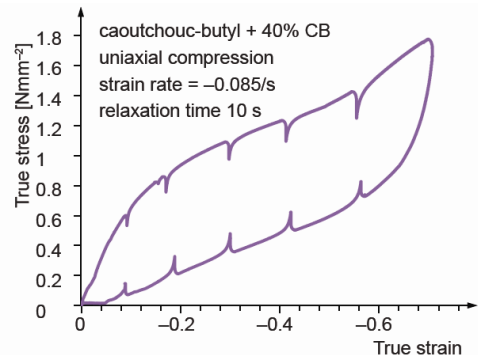


Figure 6. Stress relaxation test of the rubber sample

Based on the performed experiments, the model parameters for the rubber compound TG-B-712 were obtained during the optimization procedure in the MCalibration software. The following material parameters were obtained: $\mu_A^0 = 0.8$, $\lambda_{A_n}^{lock} = 5.23$, $\mu_B^0 = 9.87$, $\lambda_B^{lock} = 5.23$, $K = 565$, $\xi = 2.47$, $C = -0.9$, $m = 12.64$, $r = 120.74$, $\dot{U} = 4.14$, $\beta = 0.00054$, $\alpha_{min} = 0.92$, and $b = 0.34$. Figure 7 shows the comparison between experimentally obtained and predicted behavior with optimized material parameters. It is clear from fig. 7 that Bergstrom-Boyce-Mullins model gives very good prediction of behavior with selected material parameters.

Prediction of temperature distribution

As parameters of rubber constitutive model were determined, the next step in the proposed procedure was the static structural analysis of the spring where heat generation due to hyste-

resis was the object of verification study. Due to the symmetry of the specimen and the load only one quarter of the model was considered. The finite element model (fig. 8) was preliminary meshed with 3-D solid hex mesh and then refined for rubber part at its boundary surfaces.

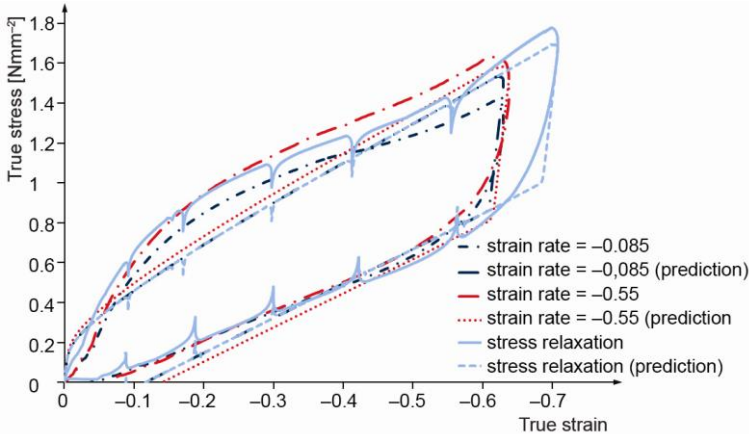


Figure 7. Comparison between experimentally obtained and predicted behaviour

The mesh refinement of the rubber part converted the hex meshing of the rubber part to the tetrahedral mesh. Although solid tetrahedral mesh is usually not recommendable due to lower convergence rates and higher degree of freedom (DOF) than hex mesh, it is unavoidable in high deformation scenarios with high friction or bonded contact conditions.

The high deformation simulations with hex dominant mesh showed that element distortion at bonded or high friction contacts of rubber metal parts is inevitable, which severely hampers the simulation accuracy. Finite element model consisted of 8134 nodes which formed 1500 3-D SOLID 185 [18] finite elements.

Due to the previously mentioned approximation of interface between the rubber and the compression plates, the contact between the compression plates and rubber specimen was defined as bonded. The rubber specimen was compressed at the same strain rate as used in the experiment to the final compression of 43%.

Figure 9 shows the comparison of load-deflection curves obtained by simulation and experimentally, and it is clear that the predicted sample behavior has a very good resemblance

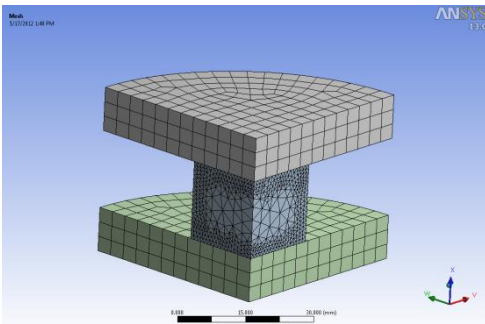


Figure 8. The FE model used in verification process

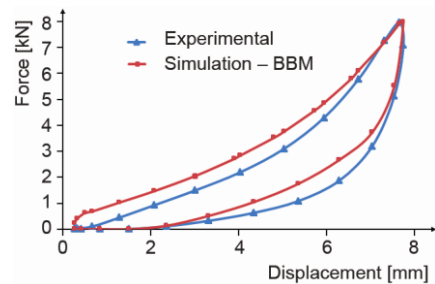


Figure 9. Comparison between experimentally obtained and predicted behavior during dynamic specimen loading

Table 2. The results of the static hysteresis test

	E_T , J	E_D , J	I , %
Experiment	20.1	11.92	40.87
Simulation	23.6	12.80	46.69

Table 3. Parameters used for heat transfer simulation [3, 6, 19]

Parameter	Value
Rubber density [kgm^{-3}]	1000
Stefan-Boltzmann constant [$\text{Wm}^{-2}\text{K}^{-4}$]	$5.67 \cdot 10^{-8}$
Steel specific heat capacity [$\text{Jkg}^{-1}\text{K}^{-1}$]	434
Rubber specific heat capacity [$\text{Wkg}^{-1}\text{K}^{-1}$]	1700
Steel conductivity coefficient [$\text{Wm}^{-1}\text{K}^{-1}$]	60.5
Rubber conductivity coefficient [$\text{Wm}^{-1}\text{K}^{-1}$]	0.238
Convective heat transfer coefficient from steel to air [$\text{Wm}^{-2}\text{K}^{-1}$]	10
Convective heat transfer coefficient from rubber to air [$\text{Wm}^{-2}\text{K}^{-1}$]	15
Steel emissivity	0.2
Rubber emissivity	0.95

to the experimental results. Table 2 gives the comparison of the values of stored energy and hysteresis obtained both experimentally and by simulation in one cycle.

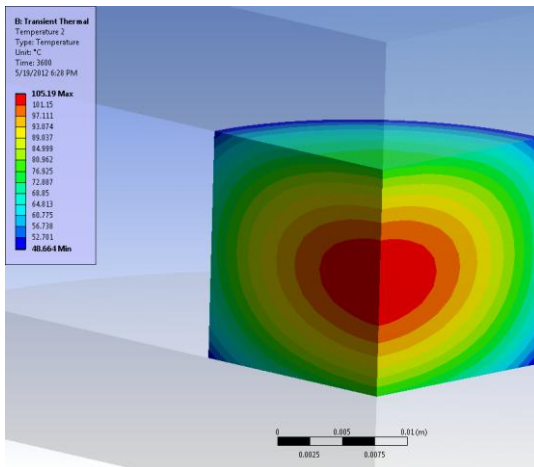
The difference between the simulated and experimentally obtained static hysteresis values is in the frame of 10 % (tab. 2), which is rather high accuracy considering the boundary accuracy criterion during the selection of rubber compound.

The predicted hysteresis values were used to determine the heat generation rate (H_G) according to eq. (1). Heat obtained generation rate (H_G) was applied as the major heat source via the internal heat generation load case. Furthermore, convection and radiation from the rubber outer surface were considered also. The values of the parameters used in the transient thermal analysis are listed in tab. 3. Parameter values were obtained from the relevant literature or predicted based on data extrapolation from the literature.

Results and discussion

The results of transient thermal simulation are shown in fig. 10. From the temperature profile the highest value is in the center of the component, which is easily understandable because the heat exchange is much quicker near the outer specimen surface. Due to sandpaper isolation, there is a minimal heat flow at the interface between the rubber specimen and the compression plates.

Figure 11 shows the comparison of the temperatures in the center of the rubber specimen obtained by experiment and simulation. There is a good agreement in maximum temperatures obtained, except the rate of the temperature rise and the time to reach an equilibrium state. The deviation in rate of the temperature rise is a consequence of

**Figure 10. Temperature distribution of rubber specimen obtained by simulation**

the strong Mullins effect exhibited by TG-B-712 rubber mixture. As unconditioned TG-B-712 specimens were used in verification procedure, the dissipated energy in the first few load cycles is significantly higher than in the case of repeatable stress-strain response characteristic to the noted rubber mixture. Higher energy dissipation due to Mullins effect leads to quicker temperature rise and shorter time to reach an equilibrium state in experimental setup. The comparison

of temperature distribution of outer rubber surface obtained by thermography and simulation is shown in fig. 12.

Good temperature match at the equilibrium-state provides confidence in the proposed procedure. The predicted temperature in equilibrium state is slightly higher due to the higher value of the predicted hysteresis loss. Higher accuracy of hysteresis prediction would lead to higher accuracy of temperature distribution prediction. Furthermore, as rubber mixture used in verification process was selected according to the boundary accuracy criterion, the obtained difference $< 5\%$ between the predicted and experimentally obtained maximal temperatures in equilibrium state further assures the reliability of the novel proposed procedure. Coupling of mechanical and thermal analysis with Maxwell visco-elastic model [4] at comparable strain has a prediction error greater than 35%, so it is clear that the proposed procedure has significantly higher prediction accuracy.

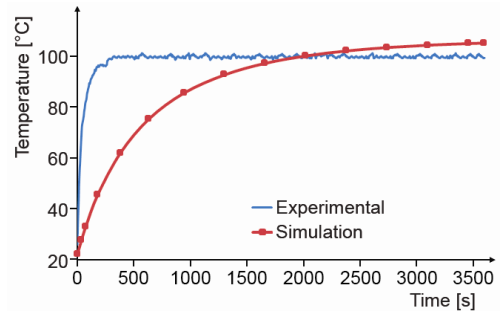


Figure 11. Comparison between experimentally temperature and predicted temperature at centre of rubber specimen

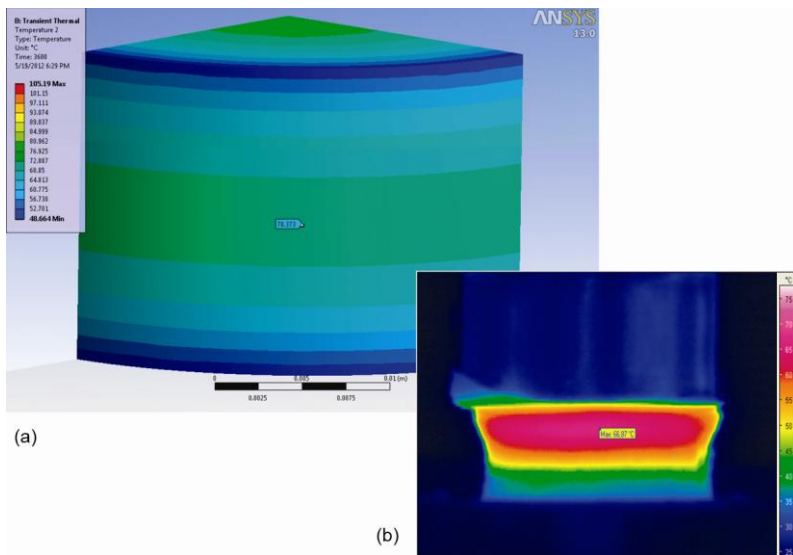


Figure 12. Comparison between thermography and predicted temperature distribution; (a) predicted temperature distribution, (b) temperature distribution obtained by thermography

By application of lifetime estimation procedures [2, 20], the temperatures obtained by the proposed procedure can be employed for the design of rubber components at the early design phase.

Conclusions

It is suggested that the following procedure should be used for the heat generation prediction: performing of static structural analysis over the required loading range, calculating the energy loss per cycle and carrying out the transient thermal simulation and evaluating the results.

The proposed procedure for prediction of heat generation in rubber or rubber-metal springs was validated during the dynamic loading of the rubber specimen. There is a good agreement between the transient thermal simulation and the experimentally obtained temperatures. It is shown that the proposed procedure is reliable and can be used to evaluate the temperature effects caused by dynamic loading in rubber or rubber-metal springs. Prediction accuracy of the proposed procedure is significantly higher than the accuracy of current prediction procedures based on visco-elastic rubber material models. The proposed procedure is highly computationally efficient and enables time integration, thus enabling the application of lifetime estimation procedures based on the obtained temperature data.

Acknowledgments

The research presented in this paper has been supported by the Serbian Ministry of Education, Science and Technological Development of the Republic of Serbia through project “Research and Development of New Generation of Wind Turbines of High Energy Efficiency”, project number TR35005.

The authors wish to thank Dr. Jorgen Bergstrom for providing access to user polymer material database (PolyUMod Library), Dr. Robert Luo for providing access to valuable literature, company TIGAR TEHNICAL RUBBER for providing the rubber specimens and Prof. Dr. Dragan Mančić, head of Thermovision laboratory from the Faculty of Electronic Engineering in Niš, for providing equipment and expertise in thermovision measurements.

Nomenclature

\mathbf{B}_A	– left Cauchy-Green tensor	\mathbf{T}	– total stress in the system
C	– material constant	\mathbf{T}_A	– total stress of the equilibrium network
$\dot{\mathbf{D}}_{Bi}$	– shape change rate of the time depended network	\mathbf{T}_B	– total stress of the time depended network
E_R	– absorbed energy	t	– time
E_D	– dissipated energy	\hat{U}	– material constant
erf	– error function	U_{dev}	– current deviatoric strain energy density
E_T	– total mechanical energy	U_{dev}^{max}	– evolving max. deviatoric strain energy
\mathbf{F}	– deformation gradient	U_{dev}^{min}	– evolving min. deviatoric strain energy
\mathbf{F}_A	– deformation gradient of the equilibrium network	<i>Greek symbols</i>	
\mathbf{F}_B	– deformation gradient of the time depended network	α_{min}	– material constant
\mathbf{F}_{Be}	– elastic deformation gradient of the time depended network	β	– material constant
\mathbf{F}_{Bi}	– inelastic deformation gradient of the time depended network	$\dot{\gamma}_0$	– dimensional consistency constant
H_G	– heat generation rate	$\dot{\gamma}_B$	– effective creep rate
I	– static hysteresis	η	– internal state variable
\mathbf{I}	– unit tensor	τ_{cut}	– cut off stress
K	– bulk modulus	λ_A^{lock}	– limiting stretch of the equilibrium network
\mathcal{L}	– Langevin function	λ_B^{lock}	– limiting stretch of the time depended network
m	– material constant	λ_i	– principal stretches
\mathbf{N}_B	– direction of the relaxed configuration driving stress	μ_{Be}^0	– initial shear modulus of the elastic part of time depended network
R	– ramp function	μ_A^0	– initial shear modulus of the equilibrium network
r	– material constant	$\hat{\tau}_B$	– material constant

References

- [1] Miltenović, V., *Machine elements – Design, Calculation, Application* (in Serbian), Mechanical Engineering Faculty, University of Niš, Niš, Serbia, 2009
- [2] Woo, C. S., Park, H. S., Useful Lifetime Prediction of Rubber Component, *Engineering Failure Analysis*, 18 (2011), 7, pp. 1645-1651
- [3] Pešek, L. *et al.*, FEM Modeling of Thermo-Mechanical Interaction in Pre-Pressed Rubber Block, *Engineering Mechanics*, 14 (2007), 1/2, pp. 3-11
- [4] Johnson, A. R., Chen, T.-Z., Approximating Thermo-Viscoelastic Heating of Largely Strained Solid Rubber Components, *Computer Methods in Applied Mechanics and Engineering*, 194 (2005), 2-5, pp. 313-325
- [5] Park, D. M. *et al.*, Heat Generation of Filled Rubber Vulcanizates and its Relationship with Vulcanizate Network Structures, *European Polymer Journal*, 36 (2000), 11, pp. 2429-2436
- [6] Luo, R. K. *et al.*, A Method to Predict the Heat Generation in a Rubber Spring Used in the Railway Industry, *Proceedings*, Institution of Mechanical Engineers, Part F: *Journal of Rail and Rapid Transit*, 219 (2005), 4, pp. 239-244
- [7] Lin, Y.-J., Hwang, S.-J., Temperature Prediction of Rolling Tires by Computer Simulation, *Mathematics and Computers in Simulation*, 67 (2004), 3, pp. 235-249
- [8] Bergstrom, J. S., Constitutive Modeling of Elastomers – Accuracy of Predictions and Numerical Efficiency, <http://www.polymerfem.com>
- [9] Stamenković, D. *et al.*, Development and Validation of Electro Locomotives Primary Suspension Rubber-Metal Elements, *Proceedings*, XIV Scientific-expert conference on railways – RAILCON '10, Niš, Serbia, 2010, pp. 79-83
- [10] Bergstrom, J. S., Boyce, M. C., Constitutive Modeling of the Large Strain Time-Dependent Behavior of Elastomers, *Journal of the Mechanics and Physics of Solids*, 46 (1998), 5, pp. 931-954
- [11] Arruda, E. M., Boyce, M. C., A Three-Dimensional Constitutive Model for the Large Stretch Behavior of Rubber Elastic Materials, *Journal of the Mechanics and Physics of Solids*, 41 (1993), 2, pp. 389-412
- [12] Bergstrom, J. S., PolyUMod – A Library of Advanced User Materials, Veryst Engineering, LLC, Needham, Mass, USA, 2012
- [13] Bergstrom, J. S., Large Strain Time-Dependent Behavior of Elastomeric Materials, Ph. D. thesis, Massachusetts Institute of Technology, Cambridge, Mass., USA, 1999
- [14] Rațiu, S., *et al.*, Numerical Simulation of Thermal Transfer in Flame Heated Ovens, *Proceedings on CD*, 11th International Symposium of Interdisciplinary Regional Research, Hungary-Romania-Serbia, Szeged, Hungary, 2010, T205
- [15] Luukkonen, A., *et al.*, Heat Generation in Dynamic Loading of Hybrid Rubber-Steel Composite Structure, *Proceedings*, 17th International Committee on Composite Materials conference, Edinburgh, Scotland, 2009
- [16] Stamenković, D., Milošević, M., Friction at Rubber-Metal Springs, *Proceedings*, 11th International Conference on Tribology – SERBIATRIB '09, Belgrade, Serbia, 2009, pp. 215-219
- [17] Korunović, N., *et al.*, Finite Element Analysis of a Tire Steady Rolling on the Drum and Comparison with Experiment, *Strojniški vestnik – Journal of Mechanical Engineering*, 57 (2011), 12, pp. 888-897
- [18] ***, ANSYS Release 13.0 documentation
- [19] Moran, M. J., Shapiro, H. N., *Fundamentals of Engineering Thermodynamics*, John Wiley & Sons Ltd, Chichester, England, 2006
- [20] Le Saux, V., *et al.*, Fast Evaluation of the Fatigue Lifetime of Rubber-Like Materials Based on a Heat Build-Up Protocol and Micro-Tomography Measurements, *International Journal of Fatigue*, 32 (2010), 10, pp. 1582-1590